Journal of Sensor Science and Technology
Vol. 28, No. 6 (2019) pp. 345-354
http://dx.doi.org/10.5369/JSST.2019.28.6.345
pISSN 1225-5475/eISSN 2093-7563

Comparison of Drift Reduction Methods for Pedestrian Dead Reckoning Based on a Shoe-Mounted IMU

Woo Chang Jung and Jung Keun Lee+

Abstract

The 3D position of pedestrians is a physical quantity used in various fields, such as automotive navigation and augmented reality. An inertial navigation system (INS) based pedestrian dead reckoning (PDR), hereafter INS-PDR, estimates the relative position of pedestrians using an inertial measurement unit (IMU). Since an INS-PDR integrates the accelerometer signal twice, cumulative errors occur and cause a rapid increase in drifts. Various correction methods have been proposed to reduce drifts. For example, one of the most commonly applied correction method is the zero velocity update (ZUPT). This study investigated the characteristics of the existing INS-PDR methods based on shoe-mounted IMU and compared the estimation performances under various conditions. Four methods were chosen: (i) altitude correction (AC); (ii) step length correction (SLC); (iii) advanced heuristic drift elimination (AHDE); and (iv) magnetometer-based heading correction (MHC). Experimental results reveal that each of the correction methods shows condition-sensitive performance, that is, each method performs better under the test conditions for which the method was developed than it does under other conditions. Nevertheless, AC and AHDE performed better than the SLC and MHC overall. The AC and AHDE methods were complementary to each other, and a combination of the two methods yields better estimation performance.

Keywords: Pedestrian dead reckoning, Inertial measurement unit, Drift reduction, Extended Kalman filter

1. INTRODUCTION

The 3D position of an object (or person) is a physical quantity used in various fields. A GPS is commonly used to determine the position of the object [1-3]. However, a GPS is difficult to use indoors and is inaccurate when it is difficult to receive satellite signals. In addition, a GPS has a low sampling rate. Therefore, a GPS is not suitable for pedestrian position estimation, because pedestrians frequently change walking directions and are indoors most of the time [4].

Recently, due to the rapid development of sensor manufacturing technology, small and affordable inertial measurement units (IMUs) have become popular. In addition, research into pedestrian dead reckoning (PDR), which estimates the relative position of pedestrians using an IMU, has become increasingly common. Inertial navigation system-based (INS-based) PDR, hereafter INS-PDR, estimates the pedestrian position by integrating the IMU's accelerometer signal twice. Therefore, it has the disadvantage of accumulating errors rapidly in the process of integrating the accelerometer signal twice [5]. In addition, the accelerometer signal of the IMU contains a gravitational acceleration; thus, it is important to remove this gravitational acceleration. To remove the gravitational acceleration from the accelerometer signal, the attitude of the sensor must be accurately estimated. However, it is not easy to accurately estimate the attitude using the IMU under dynamic conditions, i.e., when the pedestrian is walking [6]. Additionally, since it is difficult to accurately estimate the direction in which the pedestrian is walking using only the IMU, the correction of the error in the estimation of the walking direction is directly related to the accuracy of the position estimation.

Various methods have been proposed to reduce drifts caused by accumulated integration error in the INS-PDR. The most common method is the zero velocity update method (ZUPT) [1, 7-18]. A ZUPT corrects the velocity at every step to prevent rapidly accumulating drifts, but it cannot correct the accumulating error in the estimation of position caused by the orientation error and sensor noise. In INS-PDR, not only the error in the estimation of the horizontal component of the position (horizontal position

Dept. of Mechanical Eng., Hankyong National Univ.
327 Jungang-ro, Anseong, Gyeonggi 456-749, Korea.
+Corresponding author: jklee@hknu.ac.kr
(Received : Oct. 14, 2019, Revised : Nov. 21, 2019, Accepted : Nov. 22, 2019)

error) but also the error in the estimation of the vertical component of the position (vertical position error) accumulates. Several methods have been proposed to correct this [9-12]. However, in most cases, the vertical position is corrected by limiting the walking of stairs, and the vertical position of the slope walking is not corrected. In INS-PDR, the accuracy of the walking direction estimation (i.e., heading) is directly related to the horizontal position error. The use of an IMU alone does not directly correct the heading error, so it is corrected based on assumptions. In the heuristic drift elimination (HDE) method, pedestrians are assumed to walk primarily along the walls or corridors of buildings. It is also assumed that the interior/exterior interfaces of structures are generally perpendicular. The HDE sets the dominant direction for the indoor structure and corrects the heading in the near dominant direction [13]. Several methods that are based on the HDE method, such as iHDE [14], MiHDE [15], and AHDE [16], have been proposed. These methods commonly are limited, because they can correct errors in the heading only when the pedestrian is walking in a straight line. A heading correction method using map information has been proposed [17]. This method corrects the pedestrian's heading by comparing the map information with the heading of the pedestrian, assuming that pedestrians walk along the walls of a building. Another heading correction method involves estimating the heading by constructing a virtual multipath [18]. A method in which the stride length is estimated to reduce the moving distance error for each step has been proposed [19-21]. The performance of these methods is dependent upon the accuracy of the stride length estimation. Therefore, the error may increase when the stride length is incorrectly estimated. Most IMU-based methods can somewhat reduce drifts with some assumptions.

Various methods have been proposed that combine IMUs with other sensors to correct drifts. Some of these combine IMUs with identification devices to determine the position of pedestrians [22-24]. Typically, beacons, radio frequency identification, and ultrasonic sensors are used. These methods can determine the position of the user and can inhibit position accumulation errors occurring in the PDR. However, in order to use these methods, the user must establish the environment in which they are used. In radio frequency identification, three or more radio wave identification devices must be installed in the space to obtain accurate position information. The magnetometer uses the earth's magnetic field to estimate the heading of pedestrians [25-27]. Accordingly, magnetometers are frequently used with IMUs that cannot directly estimate the heading. However, they are sensitive to the surrounding magnetic fields, and large errors can result from their use in a magnetically heterogeneous space.

In this study, the features of four existing INS-PDR methods that rely on shoe-mounted IMUs were investigated, and their performances under various conditions were compared. The selected methods consist of the vertical position correction method [9], the stride length correction method [19], and the advanced HDE method AHDE [16]. We were also able to include the magnetometer-based heading correction method [25] in our study. In general, a magnetometer is used to estimate the heading, and most IMUs have embedded magnetometers. The same extended Kalman filter (EKF) was used in all the methods to ensure an accurate comparison.

2. METHODS

The EKF used in the experiments is based on that proposed in [25]. The error state vector of the EKF is $\delta\mathbf{x} = [\delta\boldsymbol{\varphi} \;\; \delta\boldsymbol{\omega}_b \;\; \delta\mathbf{p} \;\; \delta\mathbf{v} \;\; \delta\mathbf{a}_b]^T$. Here, $\delta\boldsymbol{\varphi}$ is the orientation error expressed in terms of the roll (α), pitch (β), and yaw (γ) of the Euler angle; $\delta\boldsymbol{\omega}_b$ and $\delta\mathbf{a}_b$ represent the gyroscope and accelerometer biases, respectively, and $\delta\mathbf{p}$ and $\delta\mathbf{v}$ represent the position and velocity errors, respectively. The yaw in the Euler angle represents the heading.

2.1 EKF for pedestrian dead reckoning

The INS-PDR proposed in [25] estimates the position and orientation of pedestrian shoes by integrating the accelerometer and gyroscope signals from the IMU. Each sensor is modeled as

$$ {}^{S}\mathbf{a}_k = {}^{S}\mathbf{y}_{A,k} - \delta\mathbf{a}_{b,k} - {}^{S}\mathbf{g} \tag{1.a}$$

$$ {}^{S}\boldsymbol{\omega}_k = {}^{S}\mathbf{y}_{G,k} - \delta\boldsymbol{\omega}_{b,k} \tag{1.b}$$

where ${}^{S}\mathbf{y}_{A,k}$ and ${}^{S}\mathbf{y}_{G,k}$ represent the accelerometer and gyroscope signals in the k^{th} frame with respect to the sensor coordinate $\{S\}$, respectively (recall that the sensor is attached to the shoe), and ${}^{S}\mathbf{g}$ represents the gravity with respect to the sensor coordinate. ${}^{S}\mathbf{a}_k$ represents the acceleration with the gravity and the bias are removed from the accelerometer signal, and ${}^{S}\boldsymbol{\omega}_k$ represents the angular velocity with the bias removed from the gyroscope signal. ${}^{I}_{S}\mathbf{R}$, the orientation of the sensor coordinate $\{S\}$ with respect to the inertial coordinate $\{I\}$, is updated using ${}^{S}\boldsymbol{\omega}_k$.

$$ {}^{I}_{S}\mathbf{R}_{k|k-1} = {}^{I}_{S}\mathbf{R}_{k-1|k-1} \cdot \frac{2\mathbf{I}_{3\times3} + \left[{}^{S}\boldsymbol{\omega}_k \times\right]\Delta t}{2\mathbf{I}_{3\times3} - \left[{}^{S}\boldsymbol{\omega}_k \times\right]\Delta t} \tag{2}$$

where Δt represents the sampling time and $\left[{}^{S}\boldsymbol{\omega}_k \times\right]$ denotes the

Table 1. Summary of the drift reduction methods

	Sensor	Target to be corrected	Assumption	Limitation
AC	IMU only	Vertical position	Constant and given stair height	Working only for stair and level walking
SLC	IMU only	Step length	-	Dependent on accuracy of step length estimation
AHDE	IMU only	Heading	Straight walking	Working only for straight walking
MHC	IMU+magnetometer	Heading	-	Sensitive on magnetic homogeneity

skew symmetric matrix of ${}^{S}\boldsymbol{\omega}_k$. The subscript $k|k-1$ denotes *a priori* at the current frame, and $k-1|k-1$ denotes *a posteriori* at the previous frame.

The position of the pedestrian is updated by integrating the acceleration with respect to the inertial coordinate $\{I\}$. In this case, the integrated acceleration is the gravity removed acceleration using ${}^{I}_{S}\mathbf{R}_{k|k-1}$.

$$ {}^{I}\mathbf{a}_k = {}^{I}_{S}\mathbf{R}_{k|k-1}\left({}^{S}\mathbf{y}_{A,k} - \delta\mathbf{a}_{b,k}\right) - {}^{I}\mathbf{g} \tag{3}$$

where ${}^{I}\mathbf{g} = \begin{bmatrix}0 & 0 & g\end{bmatrix}^T$, and the magnitude of gravity g is 9.8 m/s^2. The recursive equation that is used to update the position of the pedestrian is

$$ {}^{I}\mathbf{v}_{k|k-1} = {}^{I}\mathbf{v}_{k-1|k-1} + {}^{I}\mathbf{a}_k\,\Delta t \tag{4.a}$$

$$ {}^{I}\mathbf{p}_{k|k-1} = {}^{I}\mathbf{p}_{k-1|k-1} + {}^{I}\mathbf{v}_k\,\Delta t \tag{4.b}$$

${}^{I}\mathbf{p}_{k|k-1}$, ${}^{I}\mathbf{v}_{k|k-1}$, and ${}^{I}_{S}\mathbf{R}_{k|k-1}$ denote the predicted values updated by integration. They are corrected using the EKF. The corrected ${}^{I}\mathbf{p}_{k|k}$, ${}^{I}\mathbf{v}_{k|k}$ and ${}^{I}_{S}\mathbf{R}_{k|k}$ are obtained from Eq. (5).

$$ {}^{I}\mathbf{p}_{k|k} = {}^{I}\mathbf{p}_{k|k-1} - \delta\mathbf{p}_k \tag{5.a}$$

$$ {}^{I}\mathbf{v}_{k|k} = {}^{I}\mathbf{v}_{k|k-1} - \delta\mathbf{v}_k \tag{5.b}$$

$$ {}^{I}_{S}\mathbf{R}_{k|k} = \frac{2\mathbf{I}_{3\times3} - [\delta\boldsymbol{\varphi}_k\times]\Delta t}{2\mathbf{I}_{3\times3} + [\delta\boldsymbol{\varphi}_k\times]\Delta t}\cdot {}^{I}_{S}\mathbf{R}_{k|k-1} \tag{5.c}$$

The transient model of the pedestrian dead reckoning EKF, based on the error state vector $\delta\mathbf{x} = \begin{bmatrix}\delta\boldsymbol{\varphi} & \delta\boldsymbol{\omega}_b & \delta\mathbf{p} & \delta\mathbf{v} & \delta\mathbf{a}_b\end{bmatrix}^T$, is as follows:

$$ \delta\mathbf{x}_{k|k-1} = \mathbf{F}_k\delta\mathbf{x}_{k-1|k-1} + \mathbf{w}_{k-1} \tag{6}$$

where $\mathbf{w}_{k-1}$ is the process noise, which has a covariance matrix of $\mathbf{Q}_{k-1} = E\left(\mathbf{w}_{k-1}\mathbf{w}_{k-1}^T\right)$, and $\mathbf{F}_k$ is a transition matrix. The transition matrix $\mathbf{F}_k$ is

$$ \mathbf{F}_k = \begin{bmatrix} \mathbf{I} & {}^{I}_{S}\mathbf{R}_{k|k-1}\Delta t & 0 & 0 & 0 \\ 0 & \mathbf{I} & 0 & 0 & 0 \\ 0 & 0 & \mathbf{I} & \mathbf{I}\Delta t & 0 \\ -\left[{}^{I}\mathbf{a}_k\times\right]\Delta t & 0 & 0 & \mathbf{I} & {}^{I}_{S}\mathbf{R}_{k|k-1}\Delta t \\ 0 & 0 & 0 & 0 & \mathbf{I} \end{bmatrix} \tag{7}$$

The measurement model that defines the relationship between the measurement vector and the state vector is

$$ \mathbf{z}_k = \mathbf{H}_k\delta\mathbf{x}_{k|k} + \mathbf{n}_k \tag{8}$$

where $\mathbf{H}_k$ denotes the observation matrix and $\mathbf{n}_k$ represents the measurement noise with covariance matrix $\mathbf{M}_k$.

The most common drift correction method used in PDR is the zero velocity update (ZUPT) method, in which the velocity drift is corrected by setting the walking velocity to zero in the stance phase. The measurement vector for the ZUPT method is $\mathbf{z}_k = \delta ZV_k = \mathbf{v}_{k|k-1} - \begin{bmatrix}0 & 0 & 0\end{bmatrix}^T$, and the observation matrix for ZUPT is $\mathbf{H}_k = \begin{bmatrix}0_{3\times3} & 0_{3\times3} & 0_{3\times3} & \mathbf{I}_{3\times3} & 0_{3\times3}\end{bmatrix}$. The ZUPT is applied to all other drift correction methods described later. In this paper, we utilize the stance phase detection method proposed in [25].

2.2 IMU-based drift reduction methods

The ZUPT is primarily used to correct for the drift in velocity, but it is limited in its ability to correct for the position and orientation drifts. In our study, we compared drift reduction methods that use an IMU. Exceptionally, the method using magnetometer is included in the comparison method.

2.2.1 Altitude correction

The altitude correction method (AC) is based on [9]. In the AC detects stair walking is detected and the vertical position is corrected. The AC is used in the stance phase and estimates the vertical displacement change Δh to distinguish walking.

$$ \Delta h = \left|h_k - h_{ZV,i-1}\right| \tag{9}$$

where, h_k denotes vertical position in the k^{th} frame, and it is $h_k = p_{z,k}$,where $\mathbf{p}_k = \begin{bmatrix}p_{x,k} & p_{y,k} & p_{z,k}\end{bmatrix}^T$. $h_{ZV,i-1}$ denotes the vertical position of the pedestrian in the stance phase at the i-1$^{\text{th}}$ step (previous step). The threshold value h_{th} determines the presence of stairs, and the vertical displacement is determined by comparing h_k and $h_{ZV,i-1}$.

$$h_{AC} = \begin{cases} h_{ZV,i-1} + h_{stair} & \text{, if } \Delta h > h_{th} \,\&\, h_k > h_{ZV,i-1} \\ h_{ZV,i-1} - h_{stair} & \text{, if } \Delta h > h_{th} \,\&\, h_k < h_{ZV,i-1} \\ h_{ZV,i-1} & \text{, otherwise} \end{cases} \tag{10}$$

where, h_{AC} is the vertical position estimated by AC and h_{stair} is the height of the steps. The vertical position of the i^{th} step $h_{ZV,i}$ is updated to the vertical position h_k at the end of the stance phase. The vertical position error is defined by $\delta h_k = h_k - h_{AC}$. The measurement model used in the AC method is

$$\mathbf{z}_k = \begin{bmatrix} \delta h_k \\ \delta ZV_k \end{bmatrix}, \ \mathbf{H}_k = \begin{bmatrix} 0_{1\times3} & 0_{1\times3} & [0 \ \ 0 \ \ 1] & 0_{1\times3} & 0_{1\times3} \\ 0_{3\times3} & 0_{3\times3} & 0_{3\times3} & \mathbf{I}_{3\times3} & 0_{3\times3} \end{bmatrix} \tag{11}$$

The AC only corrects for errors in the vertical position due to stair walking. It does not correct for these errors when the pedestrian walks on slopes. In addition, the height of the stairs must be known and constant.

2.2.2 Step length correction

The step length correction method (SLC) corrects the moving distance error for one step by estimating the stride length using a method that is does not rely upon acceleration integration. The SLC considered in this study is based on the proposed method in [19], which estimates the stride length L using the maximum and minimum values of the accelerometer signals during one step. The stride estimation method is modeled by

$$L = c_1 \sqrt[4]{A_{\max} - A_{\min}} + c_2 (A_{\max} - A_{\min}) \tag{12}$$

where $A_{\max}$ and $A_{\min}$ represent the maximum and minimum values of the magnitude of the accelerometer signal during one step. c_1 and c_2 are the stride length estimation parameters, which vary from person to person. The error of the stride length δSL_k is as follows:

$$\delta SL_k = \mathbf{p}_{step,k} - \frac{L_k}{\left\| \mathbf{p}_{step,k} \right\|} \cdot \mathbf{p}_{step,k} \tag{13}$$

where $\mathbf{p}_{step,k}$ denotes the horizontal distance for one step in the k^{th} frame, i.e., $\mathbf{p}_{step,k} = \begin{bmatrix} p_{x,k} & p_{y,k} \end{bmatrix}^T - \begin{bmatrix} p_{x,i-1} & p_{y,i-1} \end{bmatrix}^T$. The SLC measurement model is

$$\mathbf{z}_k = \begin{bmatrix} \delta SL_k \\ \delta ZV_k \end{bmatrix}, \ \mathbf{H}_k = \begin{bmatrix} 0_{2\times3} & 0_{2\times3} & [\mathbf{I}_{2\times2} \ \ 0_{2\times1}] & 0_{2\times3} & 0_{2\times3} \\ 0_{3\times3} & 0_{3\times3} & 0_{3\times3} & \mathbf{I}_{3\times3} & 0_{3\times3} \end{bmatrix} \tag{14}$$

In the SLC, the horizontal distance is corrected by the estimated stride length. Since the stride length estimated from Eq. (12) has errors, the horizontal distance estimation error cannot be completely eliminated by the SLC.

2.2.3 Heuristic drift elimination

In the heuristic drift elimination method (HDE), most of the building walls and interior corridors are assumed to be straight and perpendicular to each other [13]. Based on this assumption, HDE sets eight dominant directions (0°, 45°, 90°, … , 315°) and corrects the heading if it is determined that the pedestrian is straight walking in This study considers the advanced heuristic drift elimination method (AHDE) proposed in [16]. The AHDE method uses linear regression to determine if the walking direction is for 6 steps and corrects the heading if pedestrian walks straight and dominant direction. Additionally, if the pedestrian walks in a straight line but not dominant, AHDE corrects the bias in the gyroscope signal. The cost function C for determining whether the walking direction is in a straight line is the sum of perpendicular distances of 6 steps from the linear function representing the walking direction for 6 steps.

$$C = \sum_{j=i-5}^{i} \left(\frac{\left| p_{y,j} - \left(a + b\, p_{x,j} \right) \right|}{\sqrt{1 + b^2}} \right)^2 \tag{15}$$

where $p_{x,j}$ and $p_{y,j}$ represent the x- and y-axis positions at the j^{th} step, respectively. a and b are defined in [16]. After calculating the cost function C, a threshold for the cost function th_c is set to determine whether the walking direction is straight, i.e., it is straight if $\min(C) < th_c$.

If the walking direction is straight for six consecutive steps in a row, it is determined whether the walking direction is the dominant direction by the heading error of the AHDE $\delta\gamma_{line}$ ($= \gamma_{line} - \gamma_{dominant}$), i.e., dominant straight if $g\gamma_{line} < th_d$. Here, γ_{line} represents the heading obtained from linear regression, and $\gamma_{dominant}$ represents the dominant direction closest to the walking direction. th_d denotes the threshold for determining whether the direction is dominant.

If it is determined that the pedestrian is walking straight and along one of the dominant directions, the measurement model is

$$\mathbf{z}_k = \begin{bmatrix} \delta\gamma_{line,k} \\ \delta ZV_k \end{bmatrix}, \ \mathbf{H}_k = \begin{bmatrix} [0 \ \ 0 \ \ 1] & 0_{1\times3} & 0_{1\times3} & 0_{1\times3} & 0_{1\times3} \\ 0_{3\times3} & 0_{3\times3} & 0_{3\times3} & \mathbf{I}_{3\times3} & 0_{3\times3} \end{bmatrix} \tag{16}$$

If the walk is not along one of the dominant directions, AHDE corrects $\delta\omega_{b,z}$ which is the z-axis of $\delta\boldsymbol{\omega}_b$.

$$\gamma_{walk,i} = \arctan\left(\frac{p_{y,i} - p_{y,i-1}}{p_{x,i} - p_{x,i-1}} \right) \tag{17.a}$$

$$\delta\omega_{b,z} = c_3 \frac{\gamma_{walk,i} - \gamma_{walk,i-4}}{\Delta t} \tag{17.b}$$

where $\gamma_{walk,i}$ is the walking direction for the i^{th} step, and c_3 uses the (3,3) component of ${}^{I}_{S}\mathbf{R}_{k|k-1}$ as the parameter for the bias. A walk in a straight line that is not in a dominant direction is modeled by

$$\mathbf{z}_k = \begin{bmatrix} \delta\omega_{b,z,k} \\ \delta ZV_k \end{bmatrix},\ \mathbf{H}_k = \begin{bmatrix} 0_{1\times3} & [0\ \ 0\ \ 1] & 0_{1\times3} & 0_{1\times3} & 0_{1\times3} \\ 0_{3\times3} & 0_{3\times3} & 0_{3\times3} & \mathbf{I}_{3\times3} & 0_{3\times3} \end{bmatrix} \quad (18)$$

If it is not a straight walk, it is the same as the measurement model that uses ZUPT only.

The AHDE has limitations that it cannot correct heading when pedestrian is not walking in a straight, and even if it is walking in a straight but not dominant direction, the heading cannot be corrected directly.

2.2.4 Magnetometer-based heading correction

The magnetometer can estimate the heading from the Earth magnetic field vector. Therefore, this can correct the heading error occurring in the PDR. This study used the method of the magnetometer-based heading correction (MHC) proposed in [25].

To estimate the heading in the MHC needs to convert the observation coordinate of the magnetometer signal through the roll (α) and pitch (β) of ${}^{I}_{S}\mathbf{R}_{k|k-1}$.

$${}^{I}\mathbf{y}'_{M,k} = \begin{bmatrix} \cos\beta_{k|k-1} & 0 & \sin\beta_{k|k-1} \\ 0 & 1 & 0 \\ -\sin\beta_{k|k-1} & 0 & \cos\beta_{k|k-1} \end{bmatrix} \begin{bmatrix} 1 & 0 & 0 \\ 0 & \cos\alpha_{k|k-1} & -\sin\alpha_{k|k-1} \\ 0 & \sin\alpha_{k|k-1} & \cos\alpha_{k|k-1} \end{bmatrix} {}^{S}\mathbf{y}_{M,k} \quad (19)$$

where ${}^{I}\mathbf{y}'_{M,k}$ represents the magnetometer signal obtained by converting the coordinate ${}^{S}\mathbf{y}_{M,k}$ to an inertial coordinate using the roll and pitch of ${}^{I}_{S}\mathbf{R}_{k|k-1}$. The roll is $\alpha_{k|k-1} = \arctan\left({}^{I}_{S}\mathbf{R}_{k|k-1}(3,2) \middle/ {}^{I}_{S}\mathbf{R}_{k|k-1}(3,3)\right)$, and the pitch is $\beta_{k|k-1} = -\arcsin\left({}^{I}_{S}\mathbf{R}_{k|k-1}(3,1)\right)$. The equation for estimating the heading using ${}^{I}\mathbf{y}'_{M,k}$ is

$$\gamma_{mag} = -\arctan\left({}^{I}\mathbf{y}'_{M,k}(2) / {}^{I}\mathbf{y}'_{M,k}(1)\right) - \theta_d \quad (20)$$

where γ_{mag} is the estimated heading from the magnetometer and θ_d is the dip angle in the Earth's magnetic field. The heading error $\delta\gamma_{mag,k} = \gamma_k - \gamma_{mag}$ is estimated using the MHC. The measurement model used to correct the heading error is

$$\mathbf{z}_k = \begin{bmatrix} \delta\gamma_{mag,k} \\ \delta ZV_k \end{bmatrix},\ \mathbf{H}_k = \begin{bmatrix} [0\ \ 0\ \ 1] & 0_{1\times3} & 0_{1\times3} & 0_{1\times3} & 0_{1\times3} \\ 0_{3\times3} & 0_{3\times3} & 0_{3\times3} & \mathbf{I}_{3\times3} & 0_{3\times3} \end{bmatrix} \quad (21)$$

Because the MHC method relies upon the use of a magnetometer, the heading estimation error can be increased when MHC is used in a magnetically heterogeneous environment.

2. EXPERIMENTS

To compare the performances of the PDR error reduction methods, we used MTw (Xsens Technologies B.V., Netherlands), which consists of an accelerometer, a gyroscope, and a magnetometer. The IMU was fixed in the shoelace of the right shoe and sampled at 100 Hz (see Fig. 1).

Fig. 1. Shoe-mounted IMU.

Table 2. Test conditions

	Environment	Length of the course (m)		Dominant direction	Standard deviation of $\lVert\mathbf{y}_m\rVert$ (a.u.)
		Horizontal	Vertical		
Test 1	Outdoor	200	0	Yes	0.02
Test 2	Outdoor	153.7	0	No	0.01
Test 3	Indoor	125.6	0	Yes	0.55
Test 4	Outdoor	147.4	10.2	Yes	0.29

The routes along which the pedestrian walked in each of the four experiments varied. Table 2 summarizes the conditions under which each experiment was conducted.

The first experiment was conducted outdoors, and the route along which the experiment was conducted consisted of traversing back-and-forth along a straight 100 m path (Test 1). The second experiment was also conducted outdoors, and the pedestrian walked the center circle of a football stadium (Test 2). The route started from the sideline; the pedestrian walked in the center circle twice and then returned to original position. The third experiment was conducted indoors in a heterogeneous magnetic environment (compared to the outdoor environments) (Test 3). The standard deviation of the magnetometer signal norm from the indoor experiment is 0.55 a.u., which is larger than those from the other three experiments. The fourth experiment was conducted outdoors and included a stair path (Test 4). In all experiments, the paths along which the pedestrian walked terminated at the same place at which they started.

In the EKF, all parameters except those related to the accelerometer and gyroscope were manually tuned. The covariance matrix for the process noise is $\mathbf{Q}_k = diag\left[(\sigma_a^2)_{1\times3}\quad 0_{1\times3}\quad 0_{1\times3}\quad (\sigma_g^2)_{1\times3}\quad 0_{1\times3}\right]$. Here, σ_a and σ_g are the standard deviations of the magnitude of the accelerometer and gyroscope signals, respectively, and they were measured under static conditions. The elements of the covariance matrix of the measurement noise are: $\sigma_{ZV}^2 = 10^{-2}\,\mathrm{m/s^2}$, $\sigma_{AC}^2 = 10^{-3}\,\mathrm{m}$, $\sigma_{SL}^2 = 10^{-2}\,\mathrm{m}$, $\sigma_{AHDE}^2 = 10^{-2}\,\mathrm{rad}$, and $\sigma_{Mag}^2 = 10^{-2}\,\mathrm{a.u.}$. The parameters are: $c_1 = 0.221$, $c_2 = 0.038$, $th_c = 0.5$, and $th_d = 5^\circ$. Here, c_1 and c_2 are obtained through gait experiments.

The final position error (FPE) was used to compare the performance of the methods. Here, the FPE was calculated by dividing both horizontally and vertically. The error calculated by comparing the total travel distance estimated using each method with the manually measured travel distance was used as the total travel distance error (TTDE). TTDEs were computed for the horizontal component of the travel distance—not the vertical.

3. RESULTS AND DISCUSSIONS

Table 3 shows the vertical and horizontal FPEs and the TTDEs from the four methods for each experiment. Table 3-(a) shows that for Test 1, the AC and SLC yield a horizontal FPE of over 28m. In contrast, the AHDE and MHC give an FPE of less than 1 m. Therefore, it is necessary to correct the heading to accurately estimate the horizontal position. The TTDE corresponding to the SLC is higher than that obtained using any of the other methods. This is because there are errors in the stride length estimation by the accelerometer. The vertical FPE corresponding to the SLC is high, because errors in the stride length estimation affect the vertical position estimation.

Fig. 2 shows the walking trajectory in Test 1 and a norm of magnetometer signal representing the tested magnetic environment. From the AHDE, the correction of the heading is well corrected because the path in this test is along one of the dominant directions. The MHC yields an increase in the error near the -40 m of x-direction. Therefore, a heading estimation error occurs even in an environment where the standard deviation of the magnetometer signal norm is 0.02 a.u. Since the pedestrian traveled back and forth along the same path, the starting and ending positions of the pedestrian are the same. As a result, the horizontal FPE obtained via the MHC is 0.8 m. The AC gives accurate vertical position estimation.

Table 3-(b) shows the results for Test 2, in which the path is circular. Because the path is circular, the heading correction from the AHDE is not worked. As a result, the horizontal FPE from the AHDE is the highest among the four methods. In contrast, the MHC yields the lowest horizontal FPE, because the heading correction is possible regardless of the path shape. The magnetic environment in Test 2 is the most homogeneous among those of the four experiments. For this test, the standard deviation of the magnetometer signal norm is 0.1 a.u. The difference between the walking trajectory in the MHC and the reference can be seen in Fig. 3. The figure shows that the heading estimation accuracy may actually be reduced if the magnetic disturbance is continuously applied-even though the disturbance is weak.

Table 3. Estimation errors (unit: m).

(a) Test 1	Horizontal FPE	Vertical FPE	TTDE
AC	29.0	0.0	0.4
SLC	28.2	1.0	2.3
AHDE	0.3	0.3	0.5
MHC	0.8	0.3	0.5

(b) Test 2	Horizontal FPE	Vertical FPE	TTDE
AC	5.3	0.0	1.2
SLC	6.0	1.4	3.0
AHDE	9.2	0.4	0.8
MHC	2.2	0.4	0.8

(c) Test 3	Horizontal FPE	Vertical FPE	TTDE
AC	6.8	0.0	0.8
SLC	7.1	0.3	0.4
AHDE	0.3	0.3	1.1
MHC	7.3	1.5	1.0

(d) Test 4	Horizontal FPE	Vertical FPE	TTDE
AC	13.2	0.1	1.2
SLC	13.1	0.8	13.9
AHDE	2.3	2.2	0.0
MHC	4.5	2.5	1.2

Table 3-(c) shows the results for Test 3, which was conducted indoors. Since it was done indoors, the standard deviation of the magnetometer signal norm is the largest (0.55 a.u.). Therefore, the MHC shows a significant performance degradation, and it has the largest vertical and horizontal FPE and TTDE values. Fig. 4 shows walking trajectory for Test 3. In Fig. 4-(a), one sees that the

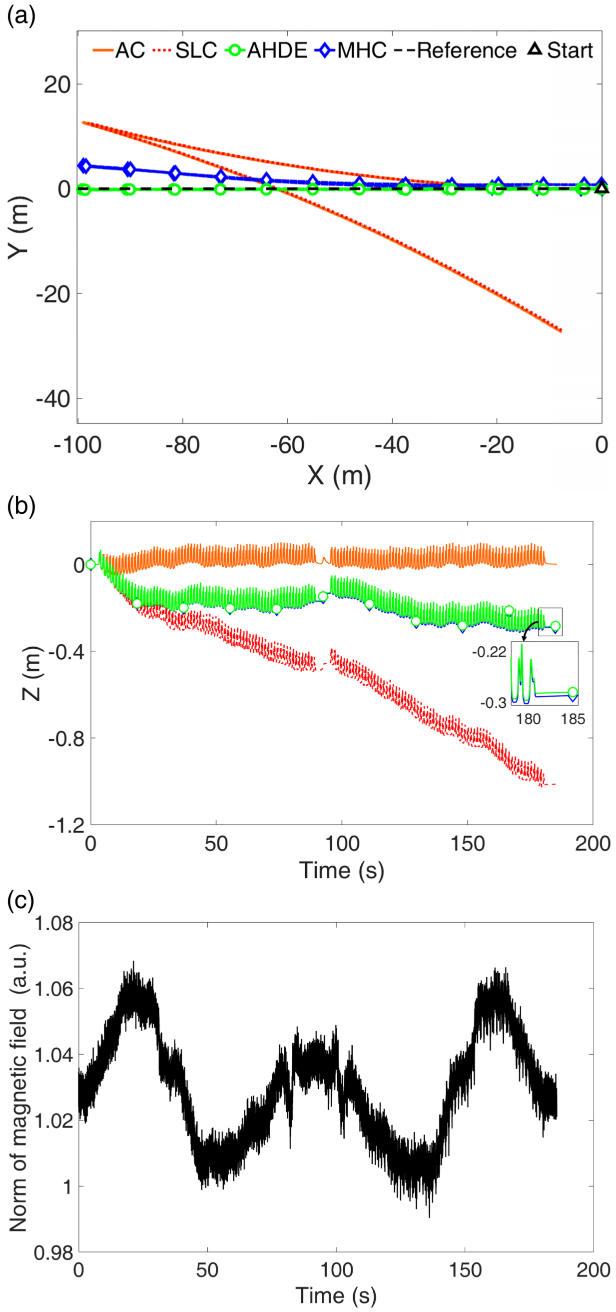

Fig. 2. Results of Test 1: (a) plan view, (b) elevation with respect to time, and (c) norm of magnetometer signals.

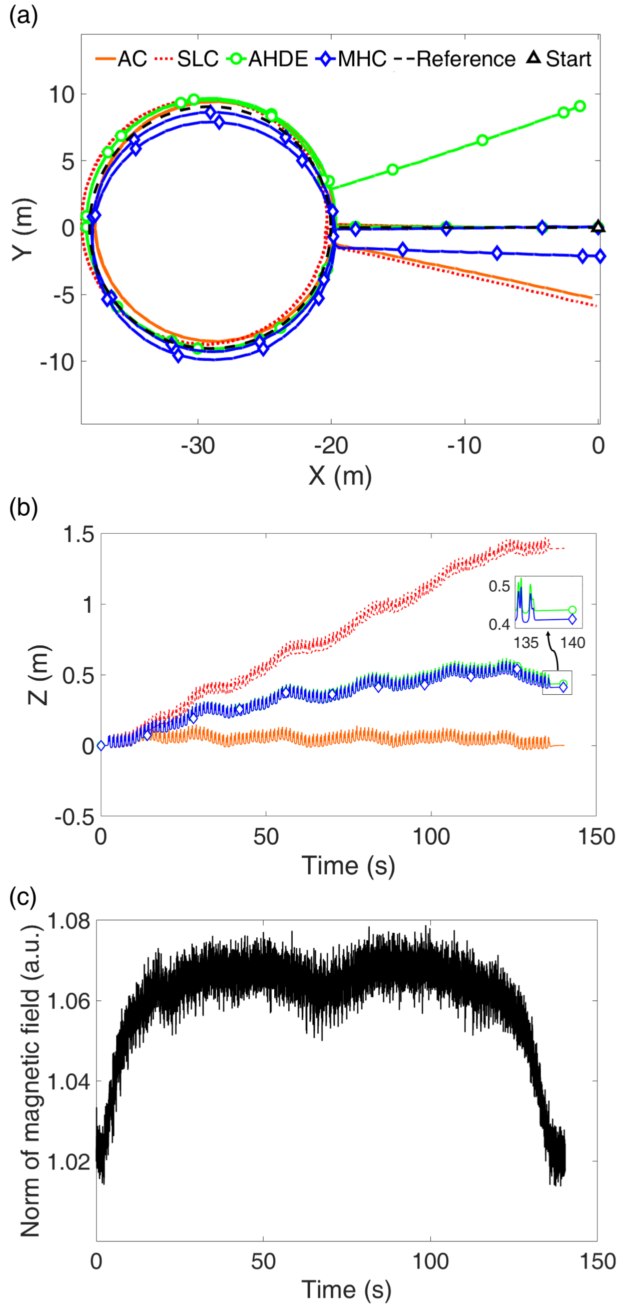

Fig. 3. Results of Test 2: (a) plan view, (b) elevation with respect to time, and (c) norm of magnetometer signals.

trajectory of the MHC varies significantly from that of the reference due to the high heading estimation error. Because the FPE only compares the starting and ending positions, there is only a 0.2 m difference between the horizontal FPE from the MHC and that from the SLC, despite the fact that the MHC and the reference have completely different trajectories. In addition, the TTDE from the MHC varies about 2.3 m from that obtained via the SLC. Therefore, verification using FPE and TTDE has a limitation that cannot account for errors occurred during walking.

Table 3-(d) shows the errors for Test 4, which includes the stairs. The AHDE shows the lowest horizontal FPE among the four methods. These values match those for Tests 1 and 3. However, Test 4 includes stair walking, so the vertical FPE error from the AHDE is 2.2 m higher than that for the other experiments. The AC shows the lowest error (0.1 m), because it corrected the vertical position of the stair walking. Fig. 5 shows the walking trajectory corresponding to Test 4 for each method. The vertical position estimation performance of the AC is shown

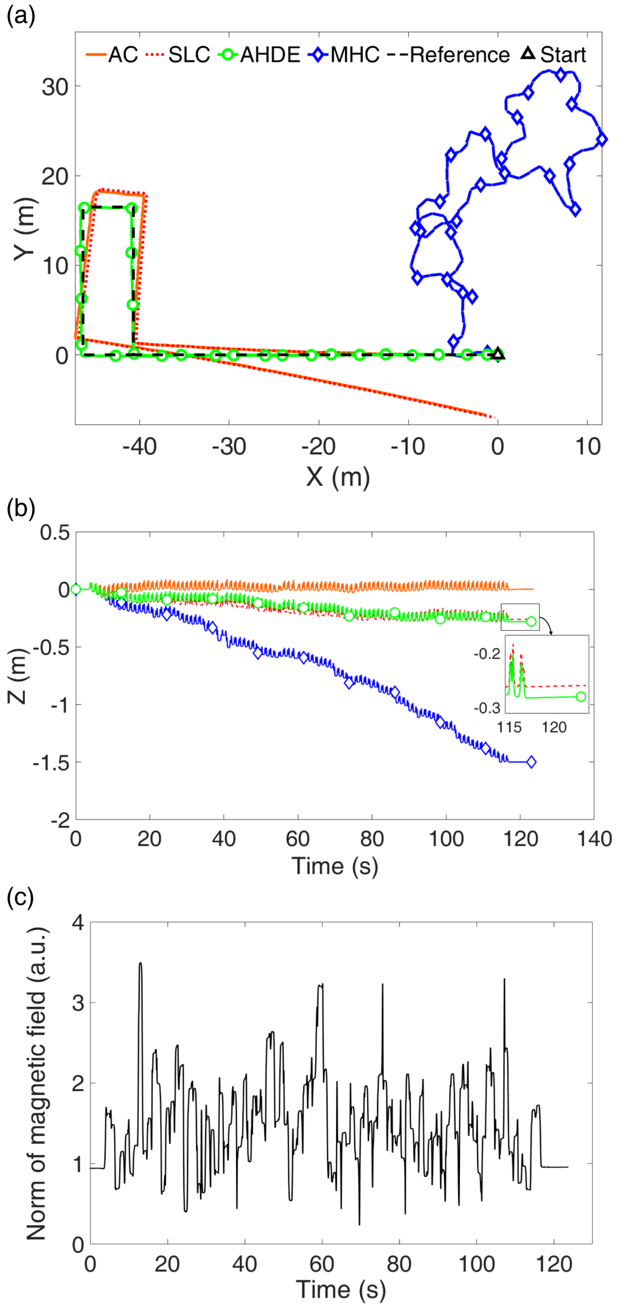

Fig. 4. Results of Test 3: (a) plan view, (b) elevation with respect to time, and (c) norm of magnetometer signals.

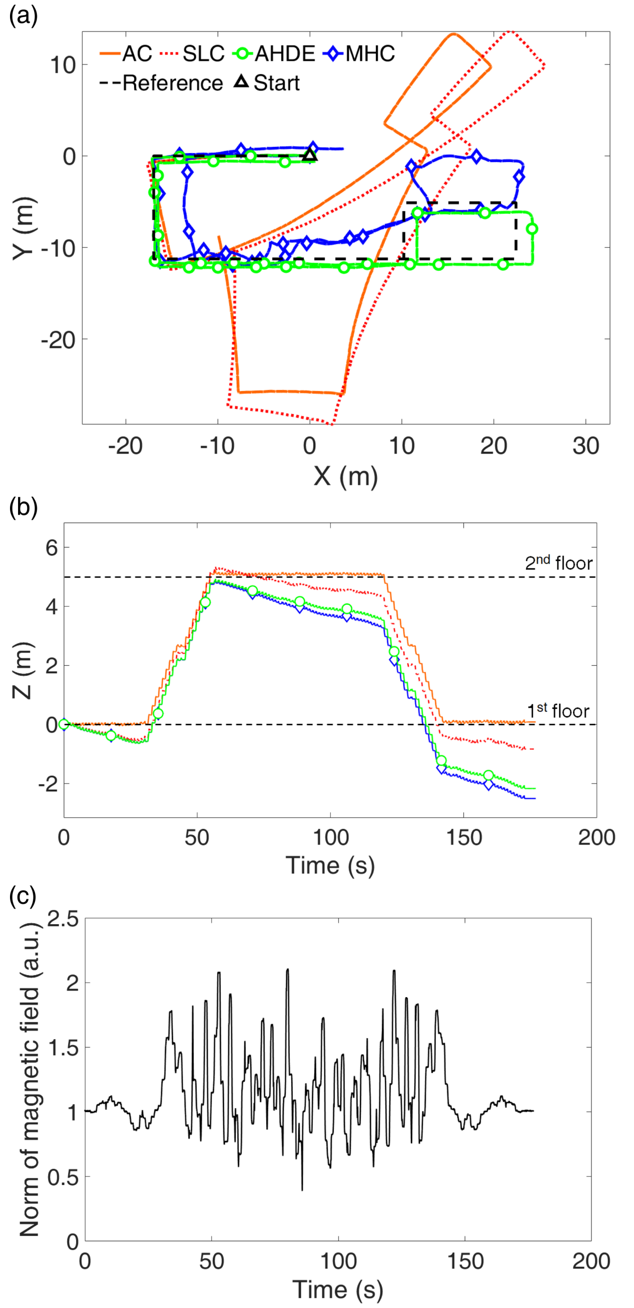

Fig. 5. Results of Test 4: (a) plan view, (b) elevation with respect to time, and (c) norm of magnetometer signals.

in Fig. 5-(b). The AC shows a constant vertical position, even though the path includes stairs. However, the AC may be used if the user knows the height of the stairs. In practice, the height of the stairs may vary both within a stairwell and from one location to the next. Therefore, the AC can only be used when the height of the stairs is known and constant.

Fig. 5-(c) shows that Test 4 was conducted outdoors in a magnetically heterogeneous environment. As a result, although the horizontal FPE from the MHC is 4.5 m, the walking trajectory in the MHC is estimated differently than it is for the reference trajectory. This is due to the heading estimation error, as shown in Fig. 5-(a). For Test 4, the TTDE from the SLC is 13.9 m, which is larger than it is for the other experiments. In the SLC, the stride length estimation uses the maximum and minimum accelerations of one step. Because Test 4 includes stairs, the actual stride length is shorter than the estimated stride length from the SLC, even though the stair walking acceleration is similar to that obtained when the path is level. Therefore, when the path involves stairs,

Table 4. Errors from the combination of AC and AHDE (unit: m)

	Horizontal FPE	Vertical FPE	TTDE
Test 1	0.1	0.0	0.4
Test 2	10.18	0.0	1.3
Test 3	0.1	0.0	0.8
Test 4	0.5	0.1	1.3

the moving distance error obtained via the SLC increases.

We examined the performance of the four selected methods by using them in four different experiments. The performance of the methods varies depending on the experimental conditions. In most of the INS-PDR, several drift reduction methods were combined to reduce the drift in the position estimation. The AC produces the lowest vertical position error, and the AHDE produces the lowest horizontal position error. In this study, we combined the AC and AHDE based on the results of the experiments. Table 4 shows the results of the combined method. In tests 1, 3, and 4, to which the AHDE method can be applied, low vertical and horizontal FPE values are obtained. In particular, the combined method produces a lower horizontal FPE than the AHDE alone does. Thus, it is necessary to combine several methods appropriately for accurate position estimation in INS-PDR.

5. CONCLUSION

In this study, the performances of four drift reduction pedestrian dead reckoning methods, which used a shoe-mounted-IMU, were evaluated. Their performances were compared by applying the methods to four experiments that were designed to clearly reveal the characteristics of the methods. Experimental results reveal that each the methods exhibits condition-sensitive performance, i.e., each method performs best under test conditions for which the method was developed (and is less effective under other conditions). The AC and AHDE perform better than the SLC and MHC do overall. In order to properly use the SLC and MHC, it is necessary to accurately estimate the parameters and consider the experimental environment. The AC and AHDE are complementary, and a combination of the two methods yields the best estimation performance.

ACKNOWLEDGMENT

This research was supported by Basic Science Research Program through the National Research Foundation of Korea (NRF) funded by the Ministry of Education (grant number: 2018R1D1A1B07042791).

REFERENCES

[1] E. Foxlin, “Pedestrian tracking with shoe-mounted inertial sensors”, *IEEE Comput. Graph. Appl.*, Vol. 25, No. 46, pp. 38-49, 2005.

[2] R. Bajaj, S. L. Ranaweera, and D. P. Agrawal. “GPS: location-tracking technology”, *Computer*, Vol. 35, No. 4, pp. 92-94, 2002.

[3] S. Godha, G. Lachapelle, and M. E. Cannon. “Integrated GPS/INS system for pedestrian navigation in a signal degraded environment”, *Proc. ION GNSS.* pp. 2151–2164, TX, USA, 2006

[4] Q. Wang, X. Chen, R. Chen, Y, Chen, and X. Zhang, “Electromyography-based locomotion pattern recognition and personal positioning toward improved context-awareness applications”, *IEEE Trans. Syst. Man Cybern. Syst.*, Vol. 43, No. 5, pp. 1216-1227, 2013.

[5] A. Brajdic and R. Harle, “Walk detection and step counting on unconstrained smartphones”, *Proc. 2013 ACM Int. Jt. Conf. on Pervasive Ubiquitous Comput.*, pp. 225-234, Zurich, Switzerland, 2013.

[6] J. K. Lee, E. J. Park, and S. N. Robinovitch, “Estimation of attitude and external acceleration using inertial sensor measurement during various dynamic conditions”, *IEEE Trans. Instrum. Meas.*, Vol. 61, No. 8, pp. 2262-2273, 2012.

[7] R. Harle, “A survey of indoor inertial positioning systems for pedestrians”, *IEEE Commun. Surv. Tutor.,* Vol. 15, No. 3, pp. 1281-1293, 2013.

[8] C. Fischer, P. Talkad Sukumar, and M. Hazas, “Tutorial: implementing a pedestrian tracker using inertial sensors”, *IEEE Pervasive Comput.*, Vol. 12, No. 2, pp. 17-27, 2013.

[9] X. Tian, J. Chen, Y. Han, J. Shang, and N. Li, “Pedestrian navigation system using MEMS sensors for heading drift and altitude error correction”, *Sens. Rev.,* Vol. 37 No. 3, pp. 270-281, 2017.

[10] A. Norrdine, Z. Kasmi, and J. Blankenbach, “Step detection for ZUPT-aided inertial pedestrian navigation system using foot-mounted permanent magnet”, *IEEE Sens. J.*, Vol. 16, No. 17, pp. 6766-6773, 2016.

[11] A. Bahillo, I. Angulo, E. Onieva, A. Perallos, and P. Fernández, “Low-cost bluetooth foot-mounted IMU for pedestrian tracking in industrial environments”, *2015 IEEE Int. Conf. on Ind. Technol. (ICIT)*, pp. 3430-3434, Seville, Spain, 2015.

[12] J. K. Lee, “A two-step Kalman/complementary filter for estimation of vertical position using an IMU-barometer system”, *J. Sens. Sci. Technol.*, Vo. 25, No. 3, pp.202-207, 2016.

[13] J. Borenstein and L. Ojeda, “Heuristic drift elimination for personnel tracking systems”, *J. Navig.*, Vol. 63, No. 4, pp. 591-606, 2010.

[14] A. R. Jiménez, F. Seco, F. Zampella, J. C. Prieto, and J.

Guevara, "Improved heuristic drift elimination (iHDE) for pedestrian navigation in complex buildings", *2011 Int. Conf. on Indoor Position. Indoor Navig.*, Guimaraes, Portugal, pp. 1-8, 2011.
[15] A. R. Jimenez, F. Seco, F. Zampella, J. C. Prieto, and J. Guevara, "Improved heuristic drift elimination with magnetically-aided dominant directions (MiHDE) for pedestrian navigation in complex buildings", *J. Locat. Based Serv.*, Vol. 6, No. 3, pp. 186-210, 2012.
[16] H. J. Ju, M. S. Lee, C. G. Park, S. Lee, and S. Park, "Advanced heuristic drift elimination for indoor pedestrian navigation", *2014 Int. Conf/ on Indoor Position. Indoor Navig. (IPIN)*, Busan, Korea, pp. 729-732, 2014.
[17] K. Abdulrahim, C. Hide, T. Moore, and C. Hill, "Aiding low cost inertial navigation with building heading for pedestrian navigation", *J. Navig*., Vol. 64, No. 2, pp. 219-233, 2011.
[18] H. Ju, S. Y. Park, and C. G. Park, "A smartphone-based pedestrian dead reckoning system with multiple virtual tracking for indoor navigation", *IEEE Sens. J.*, Vol. 18, No. 16, pp. 6756-6764, 2018.
[19] Q. Fan, H. Zhang, P. Pan, X. Zhuang, J. Jia, P. Zhang, Z. Zhao, G. Zhu, and Y. Tang, "Improved pedestrian dead reckoning based on a robust adaptive Kalman filter for indoor inertial location system", *Sensors*, Vol. 19, No. 2, pp. 294(1)-294(21), 2019.
[20] J. C. Alvarez, D. Alvarez, A. López, and R. C. González, "Pedestrian navigation based on a waist-worn inertial sensor", *Sensors*, Vol. 12, No. 8, pp.10536-10549, 2012.
[21] M. N. Muhammad, Z. Salcic, and K. I. Wang, "Indoor pedestrian tracking using consumer-grade inertial sensors with PZTD heading correction", *IEEE Sensors J.*, Vol. 18, No. 12, pp. 5164-5172, 2018.
[22] L. M. Ni, Y. Liu, Y. C. Lau, and A. P. Patil, "LANDMARC: indoor location sensing using active RFID", *Wirel. Netw.*, Vol. 10, No. 6, pp. 701-710, 2004.
[23] A. Ward, A. Jones, and A. Hopper, "A new location technique for the active office", *IEEE Pers. Commun.*, Vol. 4, No. 5, pp. 42-47, 1997.
[24] J. Hallberg, M. Nilsson, and K. Synnes, "Positioning with bluetooth", *10th Int. Conf. on Telecommun. ICT 2003*, pp. 954-958, Papeete, French Polynesia, 2003.
[25] A. R. Jiménez, F. Seco, J. C. Prieto, and J. Guevara, "Indoor pedestrian navigation using an INS/EKF framework for yaw drift reduction and a foot-mounted IMU", *2010 7th Workshop on Position. Navig. Commun*. pp. 135-143, Dresden, Germany, 2010.
[26] J. K. Lee, "A parallel attitude-heading Kalman filter without state-augmentation of model-based disturbance components", *IEEE Trans. Instrum. Meas.*, Vol. 68, No. 7, pp. 2668-2670, 2019.
[27] J. W. Song and C. G. Park, "Enhanced pedestrian navigation based on course angle error estimation using cascaded Kalman filters", *Sensors*, Vol. 18, No. 4, pp. 1281(1)-1281(20), 2018.